

# The Effect of Transverse Energy on Electronic Bound States in Heterostructure Quantum Wells

Elias Kougianos<sup>1</sup> and Saraju P. Mohanty<sup>2</sup>

<sup>1</sup>Dept of Engineering Technology, University of North Texas, Denton, TX 76203, USA.

E-mail: eliask@unt.edu

<sup>2</sup>Dept of Computer Science and Engineering, University of North Texas, Denton, TX 76203, USA.

E-mail: smohanty@cs.unt.edu

**Abstract.** Using first-order non-degenerate perturbation theory, we derive an approximate expression for the average transverse energy of electrons populating the subbands of a 2D electron gas confined in a heterostructure quantum well. We also perform detailed numerical calculations in a prototype AlGaAs/GaAs well, validate the theory and identify conditions under which this result reduces to the commonly used thermal approximation  $k_B T$ .

PACS numbers: 71.55.Eq, 73.20.-r, 73.21.Fg

Submitted to: *Semicond. Sci. Technol.*

## 1. Introduction

Quantum wells formed by the conduction and valence band edges in structures composed of dissimilar materials constitute one of the dominant features of today's electronic and optoelectronic devices [1, 2]. One of the characteristics of these wells is that they typically admit one or more bound states in which the two-dimensional electron gas (2DEG) confined within the well forms subbands [3].

The properties of the 2DEG have attracted considerable attention [4, 5] due to its role in determining the device's electronic and optoelectronic properties. One of the particular properties of the 2DEG, and the one that will be the subject of this work, is the precise form of the energy-wave vector ( $E(\mathbf{k})$ ) relation and its deviation from a simple parabolic form. In situations where the wave function (or, more precisely, the envelope function, a distinction that will be made clear in the following section) penetrates the regions outside the quantum well, this deviation can be significant.

Furthermore, we will show that the dominant factor in this deviation is not the envelope function penetration *per se* but rather the mismatch between the electron effective masses in the region of confinement and the region at which the electrons are injected into the device.

We will start by providing a short but relevant presentation of the effective-mass equation formulation for a single-band single-electron picture. We will highlight exactly where the role of the injecting region enters the picture and why the energy of the electrons injected (which uniquely determines their transverse energy) cannot be fully decoupled from the overall picture. This necessitates the calculation of relevant quantities, such as bound state energies, as functions of the transverse energy rather than as independent quantities.

Because of the computational complexity introduced by such a functional dependence, a common approximation used is to just consider these properties at a single "average" transverse energy [6, 7],  $\langle \varepsilon_{\perp} \rangle$ , which is typically taken as the average thermal energy of the 2DEG,  $k_B T$ , where  $k_B$  is Boltzmann's constant and  $T$  is the temperature of the 2DEG. In other approaches [8] the thermal energy is altogether ignored. Using standard perturbation theory techniques we will derive a more precise expression for  $\langle \varepsilon_{\perp} \rangle$  and obtain conditions under which this expression reduces to  $k_B T$ . This rigorous result allows for accurate simulations of bound states, transmission coefficients and J-V characteristics of 1-D heterostructure quantum well devices such as Resonant Tunneling Diodes (RTDs) [6, 7, 8].

Finally, using a prototype rectangular well we will perform numerical experiments and study the dependence of the bound state energies on transverse energy, provide numerical justification for our choice of perturbation theory approach and show that, within the framework of the single-band effective mass approximation, the common substitution  $\langle \varepsilon_{\perp} \rangle = k_B T$  could be in significant error.

## 2. The Effective-Mass Equation

We start by considering the general behavior of an electron in a quantum well defined by the conduction band edge of the heterostructure. Ignoring spin effects and within the free electron model, the full three-dimensional hamiltonian for a single electron is:

$$\hat{H} = \hat{T}(\hat{P}) + \hat{U}(\hat{R}), \quad (1)$$

where the kinetic energy operator  $\hat{T}$  is a function of the momentum operator  $\hat{P}$  alone, and  $\hat{U}(\hat{R})$  is the average potential that the electron is subjected to and is a function of the position operator  $\hat{R}$ .

Within the framework of the effective-mass approximation [9], the spatial periodicity of the crystal allows the effect of  $\hat{U}(\hat{R})$  in Eq. (1) to be included by simply replacing the free electron vacuum mass  $m_0$  with a position-dependent effective mass operator  $\hat{M}^*(\hat{R})$ .

The precise functional form of  $\hat{T}$  is problematic for heterostructures where the effective mass changes with position. Several different alternatives have been proposed [10, 11, 12], but we will use the Ben-Daniel form [13] due to its simplicity and manifestly Hermitian properties. Finally, we will also assume a single band (conduction) and rewrite Eq. (1) as:

$$\hat{H} = \frac{1}{2} \left( \hat{P} \frac{1}{\hat{M}^*(\hat{R})} \hat{P} \right) + \hat{E}_c(\hat{R}), \quad (2)$$

where  $\hat{E}_c(\hat{R})$  is the edge of the conduction band, and is possibly modulated by an externally applied field. The time-independent properties of the electron are then described by the envelope function  $|\Psi\rangle$  which satisfies the Schrödinger-like equation:

$$\hat{H}|\Psi\rangle = \left[ \frac{1}{2} \left( \hat{P} \frac{1}{\hat{M}^*(\hat{R})} \hat{P} \right) + \hat{E}_c(\hat{R}) \right] |\Psi\rangle = E_{tot} |\Psi\rangle \quad (3)$$

where  $E_{tot}$  is the total energy of the electron and can have both transverse and longitudinal components.

Implicit in the Hamiltonian presented in Eq. (3) is the absence of electron-phonon interactions. It has been shown the interactions of the electrons in a finite barrier quantum well with interface optical modes [14] can result in significant changes in the electron effective mass. In addition, these effects can depend strongly on the dimension of the quantum well [15]. In order to obtain simple analytical expressions and compare with previously published results [6, 7], we will ignore such effects here.

For the rest of this analysis we will assume a device with compositional variation along the  $x$  (longitudinal) axis and a very large cross-section along the  $yz$  (transverse or  $\perp$ ) plane as shown in Fig. 1. This allows us to treat the problem as truly one-dimensional. In certain situations, particularly for low-dimensional systems, such as quantum dots, this assumption may not be valid and band-edge modulation in the transverse equation would need to be incorporated in our analysis. Furthermore, space charge effects might be important at the boundaries of the injecting regions which would require the self-consistent solution of the Effective Mass and Poisson equations. These effects will also be ignored.

We have also followed the approach of Frensley [16] and considered the device under study to be an “open” quantum system: the contacts are not considered part of the device but instead serve as reservoirs continuously exchanging electrons with the device. The contacts themselves are in thermal equilibrium at all times, even if the device itself is not.

We now define the inverse effective mass operator as:

$$\hat{Q}(\hat{R}) = \frac{1}{\hat{M}^*(\hat{R})}. \quad (4)$$

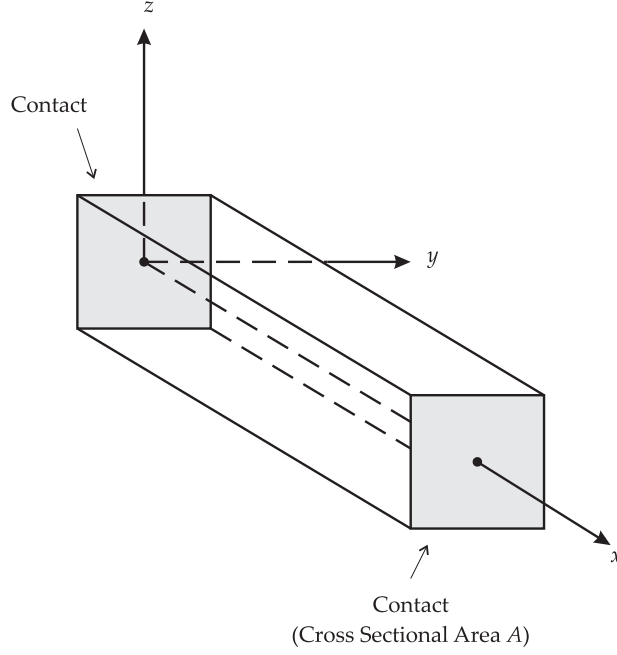


**Figure 1.** Geometry of 1-D device.  $x$  is the longitudinal direction and the  $yz$  plane is the transverse plane.

Using this definition, Eq. (3) becomes:

$$\left[ \frac{1}{2} \left( \hat{\mathbf{P}} \cdot \hat{\mathbf{Q}}(\hat{\mathbf{R}}) \cdot \hat{\mathbf{P}} \right) + \hat{E}_c(\hat{\mathbf{R}}) \right] |\Psi\rangle = E_{tot} |\Psi\rangle. \quad (5)$$

The momentum ( $\hat{\mathbf{P}}$ ) and position ( $\hat{\mathbf{R}}$ ) operators can be easily split into a direct sum of three orthogonal operators, each acting in a subspace of the complete Hilbert space and each being orthogonal to the other two. Thus we can write:

$$\hat{\mathbf{P}} = \hat{P}_x \oplus \hat{P}_y \oplus \hat{P}_z, \quad (6)$$

$$\hat{\mathbf{R}} = \hat{X} \oplus \hat{Y} \oplus \hat{Z}. \quad (7)$$

The inverse mass operator  $\hat{\mathbf{Q}}(\hat{\mathbf{R}})$ , and the band edge operator  $\hat{E}_c(\hat{\mathbf{R}})$  are functions of the position operator  $\hat{X}$  alone and do not depend on the other two position operators,  $\hat{Y}$  and  $\hat{Z}$ . We can thus write:

$$\hat{\mathbf{Q}}(\hat{\mathbf{R}}) = \hat{\mathbf{Q}}(\hat{X}) = \hat{Q}_x(\hat{X}) \oplus \hat{Q}_\perp(\hat{X}), \quad (8)$$

$$\hat{E}_c(\hat{\mathbf{R}}) = \hat{E}_c(\hat{X}), \quad (9)$$

where  $\hat{Q}_x$  and  $\hat{Q}_\perp$  are the longitudinal and transverse components of the inverse effective mass.

Eq. (5) can now be expressed as:

$$\left[ \frac{1}{2} (\hat{P}_x \oplus \hat{P}_y \oplus \hat{P}_z) \cdot \hat{\mathbf{Q}}(\hat{X}) \cdot (\hat{P}_x \oplus \hat{P}_y \oplus \hat{P}_z) + \hat{E}_c(\hat{X}) \right] |\Psi\rangle = E_{tot} |\Psi\rangle. \quad (10)$$

The presence of the operator  $\hat{Q}(\hat{X})$  “sandwiched” between the transverse components of  $\hat{P}$  prevents us from fully decoupling Eq. (5). Using the well-known commutation relations obeyed by the momentum and position operators, as well as their functions [17]:

$$[\hat{P}_\alpha, \hat{P}_\beta] = 0 \quad \text{for any } \alpha, \beta, \quad (11)$$

$$[\hat{X}, \hat{Y}] = [\hat{Y}, \hat{Z}] = [\hat{Z}, \hat{X}] = 0, \quad (12)$$

$$[\hat{Q}(\hat{X}), \hat{P}_\alpha] = \begin{cases} 0 & \text{if } \alpha = y \text{ or } z, \\ i\hbar \frac{d}{d\hat{X}} \hat{Q}_x(\hat{X}) & \text{if } \alpha = x, \end{cases} \quad (13)$$

we can rewrite Eq. (5) as:

$$\left\{ \left[ \frac{1}{2} \hat{P}_x \cdot \hat{Q}_x(\hat{X}) \cdot \hat{P}_x + \hat{E}_C(\hat{X}) \right] + \left[ \frac{1}{2} \hat{Q}_\perp(\hat{X}) \hat{P}_\perp^2 \right] \right\} |\Psi\rangle = E_{tot} |\Psi\rangle, \quad (14)$$

where  $\hat{P}_\perp^2 = \hat{P}_y^2 + \hat{P}_z^2$ .

A precise decomposition of Eq. (14) into transverse and longitudinal components is not possible because of the explicit dependence of  $\hat{Q}_\perp$  on  $\hat{X}$ . However, if we consider an adiabatic approximation wherein the longitudinal portion of the envelope function,  $|\psi_x\rangle$ , follows the changes in  $\hat{Q}_x$  rapidly while the transverse portion,  $|\psi_\perp\rangle$  adapts to the changes in the transverse effective mass  $\hat{Q}_\perp$  much more slowly, we can express the total envelope function as a tensor product of longitudinal and transverse components:

$$|\Psi\rangle \sim |\psi_x\rangle \otimes |\psi_\perp(x)\rangle. \quad (15)$$

We can thus perform a decoupling of Eq. (14) into:

$$E_x(x) |\psi_x\rangle = \left[ \frac{1}{2} \hat{P}_x \cdot \hat{Q}_x(\hat{X}) \cdot \hat{P}_x + \hat{E}_C(\hat{X}) \right] |\psi_x\rangle, \quad (16)$$

$$E_\perp(x) |\psi_\perp(x)\rangle = \left[ \frac{1}{2} \hat{Q}_\perp(\hat{X}) \hat{P}_\perp^2 \right] |\psi_\perp(x)\rangle, \quad (17)$$

where  $E_x(x) + E_\perp(x) = E_{tot} = \text{const.}$

Because both  $E_x(x)$  and  $E_\perp(x)$  are not constants these are not eigenvalue problems and cannot be used directly for the calculation of the bound states in the well. We will convert them to true eigenvalue problems if we assume that the value of the transverse energy with which the electrons are injected into the structure,  $\varepsilon_\perp$ , is known.

Towards this end we recognize Eq. (17) as a field-free wave equation. Its solution kets are characterized by the wave vector  $\mathbf{k}_\perp$ :  $|\psi_\perp(x)\rangle = |\mathbf{k}_\perp\rangle$  where:

$$\langle \mathbf{r}_\perp | \mathbf{k}_\perp \rangle = \frac{1}{\sqrt{A}} e^{i(\mathbf{k}_\perp \cdot \mathbf{r}_\perp)}, \quad (18)$$

with  $A$  an arbitrary transverse normalizing area,  $\mathbf{r}_\perp$  the transverse position vector, and

$$\frac{\hbar^2}{2m_\perp^*(x)} k_\perp^2 = E_\perp(x), \quad (19)$$

where  $m_\perp^*(x)$  is the transverse effective mass.

Since at the injecting contact:

$$\frac{\hbar^2}{2m_{\perp c}^*}k_{\perp}^2 = \varepsilon_{\perp}, \quad (20)$$

where  $m_{\perp c}^*$  is the transverse effective mass at the contact, we have:

$$E_{\perp}(x) = \frac{m_{\perp c}^*}{m_{\perp}^*(x)}\varepsilon_{\perp}, \quad (21)$$

and

$$E_x(x) = E_{tot} - E_{\perp}(x) = E_{tot} - \frac{m_{\perp c}^*}{m_{\perp}^*(x)}\varepsilon_{\perp}. \quad (22)$$

Substituting Eq. (22) back in Eq. (16), we have:

$$\left[ \frac{1}{2}\hat{P}_x \cdot \hat{Q}_x(\hat{X}) \cdot \hat{P}_x + \hat{E}_C(\hat{X}) + m_{\perp c}^*\varepsilon_{\perp}\hat{Q}_{\perp}(\hat{X}) \right] |\psi_x\rangle = E_{tot}|\psi_x\rangle. \quad (23)$$

This is now an eigenvalue problem since  $E_{tot}$  is constant.

Eq. (23) is just the single-band effective mass equation for the longitudinal envelope function, decoupled according to an adiabatic approximation. From now on, we need to only concentrate on the  $x$  direction. The effect of the transverse direction is incorporated in the transverse operator  $m_{\perp c}^*\varepsilon_{\perp}\hat{Q}_{\perp}(\hat{X})$ .

It is now clear that Eq. (23) may admit none, one, or more bound states depending on the material parameters and the width and height of the well. For the remainder of this discussion we will assume that there is at least one but otherwise unspecified number of bound states admitted, labeled by the index  $n$ . To each bound state corresponds an envelope function  $|\psi_x^n\rangle$  with energy  $E_{tot}^n$ . It is also evident that these bound states depend on the transverse energy  $\varepsilon_{\perp}$  through the action of the operator  $m_{\perp c}^*\varepsilon_{\perp}\hat{Q}_{\perp}(\hat{X})$ . Therefore, the proper way to account for the transverse features of the device is to calculate the bound state energies explicitly as a function of  $\varepsilon_{\perp}$ :  $E_{tot}^n = E_{tot}^n(\varepsilon_{\perp})$ . Properties of the device that subsequently depend on the location of the bound states (such as band bending, self consistent band edges, transmission and reflection coefficients etc.) become functions of  $\varepsilon_{\perp}$ . This severely complicates the numerical and analytical evaluation of these properties.

To simplify matters, many authors [18, 19, 20] assume that the envelope function vanishes outside the well boundaries. This allows the effect of the transverse operator  $m_{\perp c}^*\varepsilon_{\perp}\hat{Q}_{\perp}(\hat{X})$  outside the well to be ignored and since  $\hat{Q}_{\perp}(\hat{X})$  is constant inside the well, the net effect is a shift of the bound states by the amount  $(m_{\perp c}^*/m_{\perp w}^*)\varepsilon_{\perp}$ :

$$E_{tot}^n(\varepsilon_{\perp}) = E_{tot}^{n0} + \frac{m_{\perp c}^*}{m_{\perp w}^*}\varepsilon_{\perp}, \quad (24)$$

where  $m_{\perp w}^*$  is the transverse effective mass inside the well and  $E_{tot}^{n0}$  is the  $n$ -th bound state of the eigenvalue problem Eq. (23) with  $\varepsilon_{\perp} = 0$ .

Clearly this assumption fails if there is significant penetration of the envelope function outside the well, as is the case with higher states, or in the case of multiple quantum wells. Detailed  $\mathbf{k} \cdot \mathbf{p}$  energy band calculations [21, 22, 23] have incorporated spin-orbit effects and multiple bands in the Hamiltonian but for our purposes, the Single-Band Effective Mass Hamiltonian in Eq. (14) is sufficient.

If we use Eq. (20) in Eq. (24) we retrieve the familiar parabolic subband structure:

$$E_{tot}^n(\mathbf{k}_\perp) = E_{tot}^{n0} + \frac{\hbar^2 k_\perp^2}{2m_{\perp w}^*}. \quad (25)$$

Using this parabolic relation and Fermi-Dirac statistics, other authors [6, 7] replace  $\varepsilon_\perp$  with its thermal average  $k_B T$ .

In order to quantify the effects of the transverse operator more precisely, we use first-order non-degenerate perturbation theory [24]:

$$E_{tot}^n(\varepsilon_\perp) = E_{tot}^{n0} + \lambda_n \varepsilon_\perp, \quad (26)$$

where

$$\lambda_n = \langle \psi_n | m_{\perp c}^* \hat{Q}_\perp(\hat{X}) | \psi_n \rangle. \quad (27)$$

If we now concentrate on the statistics of the bound electrons, their mean transverse energy is:

$$\langle \varepsilon_\perp \rangle = \frac{\int_0^\infty \varepsilon_\perp dn_b(\varepsilon_\perp)}{\int_0^\infty dn_b(\varepsilon_\perp)}, \quad (28)$$

where  $n_b(\varepsilon_\perp)$  is the number of bound electrons at a given  $\varepsilon_\perp$ . Since there might be more than one state binding electrons of transverse energy  $\varepsilon_\perp$ , we have:

$$dn_b(\varepsilon_\perp) = \sum_n g_{2D}(E_{tot}^n(\varepsilon_\perp)) f_{FD}(E_{tot}^n(\varepsilon_\perp)) dE_{tot}^n(\varepsilon_\perp), \quad (29)$$

where the summation runs over all bound states.  $g_{2D}(E_{tot}^n(\varepsilon_\perp))$  is the density of states for a two-dimensional electron gas and is a piece-wise constant function [4]:

$$g_{2D}(E) = c \sum_n u(E - E_{tot}^n), \quad (30)$$

where  $u(x)$  is the unit step function,  $c$  is a material dependent constant and  $f_{FD}(E_{tot}^n(\varepsilon_\perp))$  is the Fermi-Dirac distribution function given by:

$$f_{FD}(E_{tot}^n(\varepsilon_\perp)) = \frac{1}{1 + \exp\left[\frac{E_{tot}^n(\varepsilon_\perp) - E_F}{k_B T}\right]}, \quad (31)$$

where  $E_F$  is the Fermi-level in the device. Using Eq. (26) in Eq. (29) we obtain the following :

$$dn_b(\varepsilon_\perp) = \sum_n \lambda_n g_{2D}(E_n(\varepsilon_\perp)) f_{FD}(E_n(\varepsilon_\perp)) d\varepsilon_\perp. \quad (32)$$

Substituting Eq. (30) and Eq. (32) in Eq. (28) we obtain:

$$\langle \varepsilon_\perp \rangle = \frac{\sum_n n \lambda_n \int_0^\infty \varepsilon_\perp f_{FD}(\varepsilon_\perp) d\varepsilon_\perp}{\sum_n n \lambda_n \int_0^\infty f_{FD}(\varepsilon_\perp) d\varepsilon_\perp}. \quad (33)$$

Using Eq. (26) and Eq. (31) in Eq. (33) we have:

$$\langle \varepsilon_{\perp} \rangle = \frac{\sum_n n \lambda_n \int_0^{\infty} \frac{\varepsilon_{\perp} d\varepsilon_{\perp}}{1 + \exp \left[ \frac{E_{tot}^{n0} + \lambda_n \varepsilon_{\perp} - E_F}{k_B T} \right]}}{\sum_n n \lambda_n \int_0^{\infty} \frac{d\varepsilon_{\perp}}{1 + \exp \left[ \frac{E_{tot}^{n0} + \lambda_n \varepsilon_{\perp} - E_F}{k_B T} \right]}}, \quad (34)$$

which finally reduces to:

$$\langle \varepsilon_{\perp} \rangle = k_B T \frac{\sum_n n \lambda_n^{-1} F_1(a_n)}{\sum_n n F_0(a_n)}. \quad (35)$$

Here  $F_j(\eta)$  is the Fermi-Dirac integral of order  $j$ :

$$F_j(\eta) = \int_0^{\infty} \frac{x^j dx}{1 + \exp(x - \eta)}, \quad (36)$$

and  $a_n$  is the normalized energy distance of the  $n$ -th unperturbed level from the Fermi-level:

$$a_n = -\frac{E_{tot}^{n0} - E_F}{k_B T}. \quad (37)$$

It is straightforward to see that, if the Fermi-level  $E_F$  lies far from all the bound levels which in turn translates to all the  $a_n$ 's being large and negative, and, in addition, the spacing of the ground level from the excited levels is large [hence  $F_j(a_1) \gg F_j(a_2) \gg \dots \gg F_j(a_n)$ ], then Eq. (35) reduces to:

$$\langle \varepsilon_{\perp} \rangle = k_B T \frac{\lambda_1^{-1} F_1(a_1)}{F_0(a_1)}. \quad (38)$$

Using the approximation  $F_j(\eta) \simeq e^{\eta} \Gamma(j+1)$  for large negative  $\eta$  [25], and assuming that the effective mass perturbation is rather small (so that  $\lambda_n \simeq 1$ ), we see that this reduces to the thermal energy  $k_B T$ .

It is seen thus that the substitution of the transverse energy with the mean thermal value  $k_B T$  is justified only if the Fermi-level is located far below the ground energy and the bound energies are sufficiently isolated from each other. If either of these conditions is violated, as would be the case in heavily doped areas or if there are severe effective mass mismatches, for example, the full expression given in Eq. (35) must be used.

### 3. Numerical Experiments

The theoretical considerations formulated in the first part of this work are tested on a prototype potential well formed by a layer of GaAs "sandwiched" between two layers of AlGaAs. In particular, we consider the rectangular well formed by the conduction band edge of a thin layer of GaAs positioned between two thick layers of  $\text{Al}_{0.3}\text{Ga}_{0.7}\text{As}$ . Electrons confined in this well will be bound if their energy corresponds to the

eigenvalues of the Hamiltonian operator for this potential profile. The parameters we use for this prototype potential well are chosen to be identical with those of [26], namely conduction band discontinuity of 0.23 eV and electron effective mass  $m^* = 0.067$  and  $m^* = 0.092$  in the GaAs and  $\text{Al}_{0.3}\text{Ga}_{0.7}\text{As}$  layers, respectively. We only consider a single conduction band ( $\Gamma$ ) and ignore the ( $L-X$ ) bands.

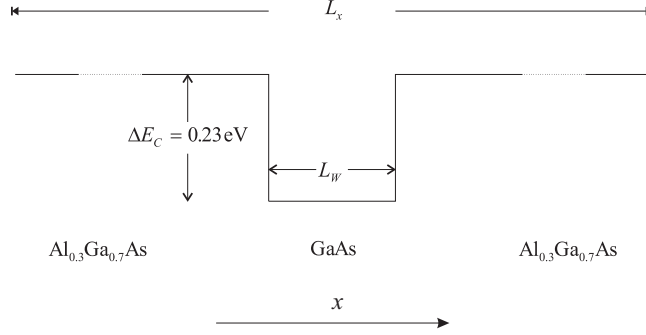


**Figure 2.** Prototype potential well geometry.  $x$  is the longitudinal direction. The transverse plane is perpendicular to it.

The geometry of the prototype well is represented in Fig. 2. It is clear that, since there is band edge modulation only along the  $x$  direction, the 2DEG will be confined there. For clarity, we define this direction as “longitudinal” for both the device and the 2DEG. Accordingly, the  $yz$  plane is considered as “transverse” for both systems.

The length of the well is  $L_W$  while the overall length of the device is  $L_x$ . We choose  $L_x = 720 \text{ \AA}$  while  $L_W = 56 \text{ \AA}$ . The restriction that  $L_W \ll L_x$  guarantees the validity of the boundary conditions [ $\psi(0) = \psi(L_x) = 0$ ] at the ends of the device.

This type of well has been studied in [20, 26]. The number  $\mathfrak{N}$  of bound states the well admits is dependent upon the material parameters and the length and depth of the well via the relationship:

$$\mathfrak{N} = 1 + \text{Int} \left[ \sqrt{\frac{2m_A^* L_W^2 |V_p|}{\pi^2 \hbar^2}} \right], \quad (39)$$

where  $m_A^*$  is the electron effective mass in GaAs and  $V_p$  is the depth of the well, 0.23 eV in our case.  $\text{Int}(x)$  is the integer part of  $x$ . For our case of  $L_W = 56 \text{ \AA}$  the well admits two bound states. Since  $L_W$  is very near the transition edge from one to two bound states (at approximately  $50 \text{ \AA}$ ), we expect the ground state to be strongly bound but the second state will be weakly bound.

In order to determine the eigenvalues and eigenvectors corresponding to the bound state energies and envelope functions, respectively, Eq. (23) is discretized using a central-difference scheme on a non-uniform grid of  $N = 180$  points. Approximately  $N/3$  points are allocated inside the well and the remaining on the flat areas of the conduction band. The procedure we follow is similar to that used in [26]. The discretized version of Eq. (23) is:

$$\sum_{j=1}^N H_{ij} \psi_j = E \psi_i, \quad (40)$$

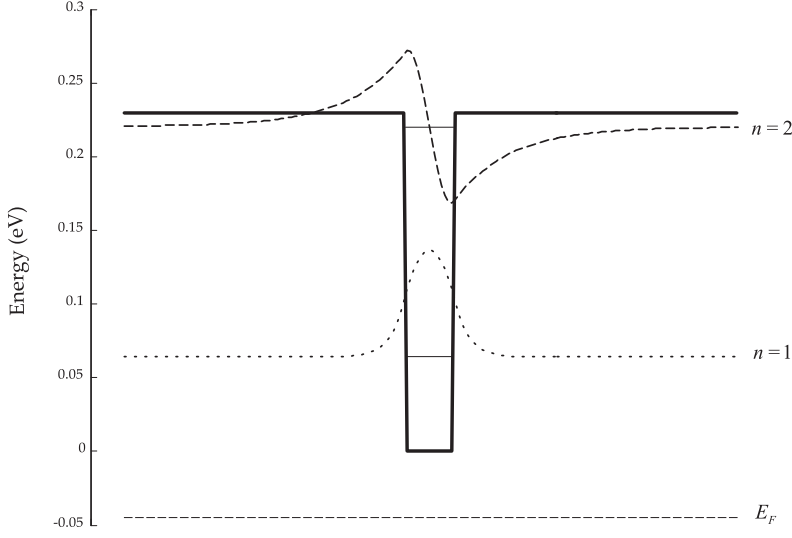


**Figure 3.** Calculated bound state energies in eV and envelope functions in arbitrary units for the prototype well. The envelope functions have been shifted vertically. The location of the Fermi-level  $E_F$  for an undoped structure is also shown.

where the discretized hamiltonian is given by:

$$H_{ij} = \begin{cases} \frac{\hbar^2}{2} \frac{2}{m_{i+1/2}^*} \frac{1}{h_{i+1}(h_i + h_{i-1})} & \text{if } j = i + 1, \\ \frac{\hbar^2}{2} \frac{2}{m_{i-1/2}^*} \frac{1}{h_{i+1}(h_i + h_{i-1})} & \text{if } j = i - 1, \\ -H_{ii+1} - H_{ii-1} + E_{Ci} + \frac{m_{\perp c}^*}{m_{\perp i}^*} & \text{if } j = i, \\ 0 & \text{otherwise.} \end{cases} \quad (41)$$

At the midpoints the effective mass is taken as simply the average at both endpoints:

$$m_{i+\frac{1}{2}}^* = \frac{m_{i+1}^* + m_i^*}{2}, \quad (42)$$

while  $h$  is the spacing between adjacent nodes on the grid:

$$h_i = x_{i+1} - x_i. \quad (43)$$

Numerically evaluating the eigenvalues and eigenvectors of the matrix  $H$  provides us then with the bound energy levels and envelope functions. We chose the origin of the energy scale to be at the bottom of the well so that any eigenvalues outside the range  $0 < E_n < 0.23$  eV are rejected.

The energy levels and envelope functions for the bound states of the prototype well for  $\varepsilon_{\perp} = 0$  are shown in Fig. 3 while the dependence of the eigenvalues on  $\varepsilon_{\perp}$  is shown in Fig. 4.

Inspection of Fig. 4 validates the assumption underlying Eq. (26), i.e. the total bound state energies depend almost linearly on the transverse energy and first

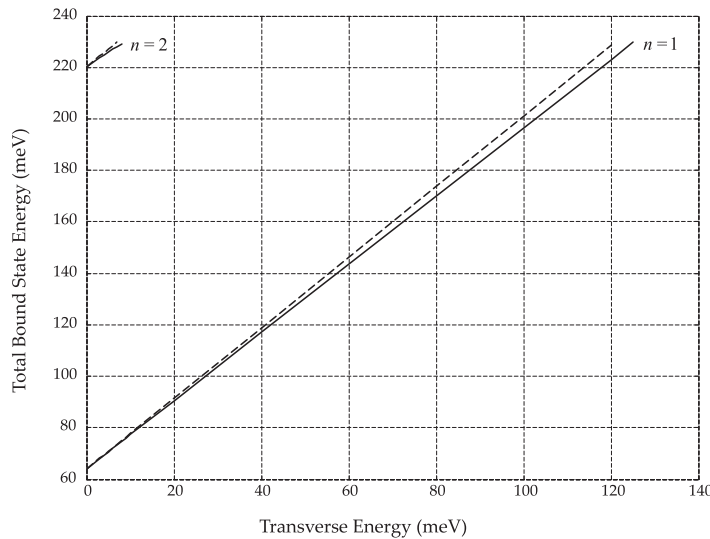


**Figure 4.** Calculated bound state energies in meV for the prototype well as a function of transverse energy. The solid lines represent numerical calculations while the dashed lines are the predictions of Eq. (24).

order perturbation theory sufficiently captures the effects of the perturbing operator. Furthermore, the results presented in Fig. 4 match with those presented in Wang *et al* [27] for the case of zero magnetic field perpendicular to the interface.

Exact numerical calculation of the sums involved in Eq. (35) for the undoped structure of Fig. 2 at room temperature (simple charge neutrality places the Fermi-level at -44.36 meV) yields:

$$\langle \varepsilon_{\perp} \rangle = 0.75k_B T, \quad (44)$$

which demonstrates that even in an undoped well with very good separation between the Fermi-level and the bound states, the error in approximating  $\langle \varepsilon_{\perp} \rangle$  with its thermal equivalent can be quite significant. In this particular case the discrepancy is due primarily to the mismatch of the effective masses in GaAs and  $\text{Al}_{0.3}\text{Ga}_{0.7}\text{As}$ . The ratio of these two effective masses, for the  $\Gamma$  band, is:

$$\frac{m_{\perp c}^*}{m_{\perp w}^*} = \frac{0.092}{0.067} = 1.37, \quad (45)$$

which from Eq. (27) implies that  $\lambda_1 \simeq 1.37$ , contrary to the assumption that  $\lambda_1 \simeq 1$ .

One final issue we wish to address is the question of how the theory and the results presented here are affected if metallic contacts with incoherent electrons coupled to the system or metallic contacts coupled to the injecting region of the system are present. As expected, these couplings will introduce additional constraints to the boundary conditions at or near the contacts and could drive the system far from equilibrium, even in steady-state. Frensley [16] has pointed out that the usual continuity boundary conditions at the contacts will be valid if the mobility is sufficiently low and that the fundamental problem lies with the time-reversibility of the boundary conditions. He then proceeds to alter this symmetry by applying time-irreversible boundary conditions to the Wigner distribution function representation

of the system. These boundary conditions model the contacts (or contact regions) as ideal reservoirs with properties similar to a blackbody. By studying a model RTD, very similar to our quantum well, he found substantially different results if he assumes a limited coherence length for the electrons (Wigner function approach,) as opposed to an infinite coherence length implied in the Schrödinger equation approach. The above mentioned effects are expected to affect the accuracy of the results presented in this paper for realistic devices, but to what extent is not known unless a fully kinetic theory model is formulated, which is beyond the scope of this work.

#### 4. Conclusion

In this work we examined the effects of the non-parabolicity for the  $E(\mathbf{k})$  relation in a two-dimensional electron gas confined within a quantum well with spatially varying effective mass.

Using a prototype well and numerical experimentation we demonstrated that the effect of the perturbing operator on the overall Hamiltonian of the electron (in a free-electron, effective mass framework) can be accurately accounted for via first-order, non-degenerate perturbation theory.

A rigorous expansion formula for the average transverse energy of the 2DEG was obtained and compared with the common approximation of using the thermal average  $k_B T$ . It is shown that this is not a good approximation, even for lightly doped or undoped devices due to the strong dependence of the perturbing Hamiltonian on the ratio of the effective masses in the different regions of the well. Since this ratio is almost always substantially different than 1, the approximation is typically in error proportional to the ratio of the effective masses.

These results can be easily generalized for multiple conduction bands and higher order perturbation theory can be used for strong deviations from parabolicity. Finally, in an extension to the theory presented here, we are currently investigating a similar approach in double quantum well structures [28].

#### Acknowledgments

The authors would like to thank the anonymous reviewers for their numerous insightful comments and suggestions.

- [1] M. Wilson, K. Kannangara, G. Smith, and M. Simmons. *Nanotechnology: Basic Science and Emerging Technologies Reviews*. Chapman and Hall/CRC, 2002.
- [2] D. F. Holcomb. Quantum electrical transport in samples of limited dimensions. *Am. J. Phys.*, 67(4):278–297, April 1999.
- [3] D. K. Ferry and S. M. Goodnick. *Transport in Nanostructures*. Cambridge University Press, Cambridge, 1997.
- [4] T. Ando, A. B. Fowler, and F. Stern. Electronic properties of two-dimensional systems. *Rev. Mod. Phys.*, 54(2):437–672, April 1982.
- [5] E. L. Ivchenko and G. E. Pikus. *Superlattices and Other Heterostructures, 2nd Ed.* Springer-Verlag, Berlin, 1997.
- [6] M. Cahay, M. McLennan, S. Datta, and M. S. Lundstrom. Importance of space-charge effects in resonant tunneling devices. *Appl. Phys. Lett.*, 50(10):612–614, March 1987.
- [7] M. O. Vassell, J. Lee, and H. F. Lockwood. Multibarrier tunneling in  $\text{Ga}_{1-x}\text{Al}_x\text{As}/\text{GaAs}$  heterostructures. *J. Appl. Phys.*, 54(9):5206–5213, September 1983.
- [8] J. Gong, X. X. Liang, and S. L. Ban. Resonant tunneling in parabolic quantum well structures under a uniform transverse magnetic field. *Chinese Physics*, 14(1):201–207, Jan. 2005.
- [9] S. Datta. *Quantum Phenomena*. Addison-Wesley, Reading, 1989.
- [10] R. A. Morrow and K. R. Brownstein. Model effective-mass Hamiltonians for abrupt heterojunctions and the associated wave-function-matching conditions. *Phys. Rev. B*, 30(2):678–680, July 1984.
- [11] R. A. Morrow. Effective-mass Hamiltonians for abrupt heterojunctions in three dimensions. *Phys. Rev. B*, 36(9):4836–4840, Sep. 1987.
- [12] R. A. Morrow. Establishment of an effective-mass Hamiltonian for abrupt heterojunctions. *Phys. Rev. B*, 35(15):8074–8079, May 1987.
- [13] D. J. BenDaniel and C. B. Duke. Space-Charge effects on electron tunneling. *Phys. Rev.*, 152(2):683–692, Dec. 1966.
- [14] E. P. Pokatilov, S. N. Klimin, S. N. Balaban, and V. M. Fomin. Polaron in a cylindrical quantum wire with finite-barrier well. *Phys. Stat. Sol. (B)*, 191(2):311–323, 1995.
- [15] G. Q. Hai, F. M. Peeters, and J. T. Devreese. Electron optical-phonon coupling in  $\text{GaAs}/\text{Al}_x\text{Ga}_{1-x}\text{As}$  quantum wells due to interface, slab, and half-space modes. *Phys. Rev. B*, 48(7):4666–4674, August 1993.
- [16] William R. Frensley. Boundary conditions for open quantum systems driven far from equilibrium. *Rev. Mod. Phys.*, 62(3):745–791, Jul 1990.
- [17] C. Cohen-Tannoudji, B. Liu, and F. Laloë. *Quantum Mechanics - Vol. 1*. John Wiley & Sons, New York, 1977.
- [18] F. Stern and W. E. Howard. Properties of semiconductor surface inversion layers in the electric quantum limit. *Phys. Rev.*, 163(3):816–835, November 1967.
- [19] F. Stern. Self-consistent results for  $n$ -type Si inversion layers. *Phys. Rev. B*, 5(12):4891–4899, June 1972.
- [20] G. Bastard and J. A. Brum. Electronic states in semiconductor heterostructures. *IEEE J. Quantum Electron.*, QE-22(9):1625–1644, September 1986.
- [21] S. Richard, F. Aniel, and G. Fishman. Energy-band structure of Ge, Si, and GaAs: A thirty-band  $\mathbf{k} \cdot \mathbf{p}$  method. *Phys. Rev. B*, 70(23):235204–(1–6), 2004.
- [22] C. W. Cheah, L. S. Tan, and G. Karunasiri. Application of analytical  $\mathbf{k} \cdot \mathbf{p}$  model with envelope function approximation to intersubband transitions in  $n$ -type III-V semiconductor  $\Gamma$  quantum wells. *J. Appl. Phys.*, 91(8):5105–5115, Apr. 2002.
- [23] N. Cavassilas, F. Aniel, K. Boujdaria, and G. Fishman. Energy-band structure of GaAs and Si: A  $sp^3s^*$   $\mathbf{k} \cdot \mathbf{p}$  method. *Phys. Rev. B*, 64(11):115207–(1–5), 2001.
- [24] C. Cohen-Tannoudji, B. Liu, and F. Laloë. *Quantum Mechanics - Vol. 2*. John Wiley & Sons, New York, 1977.
- [25] J. S. Blakemore. Approximations for Fermi-Dirac integrals, especially the function  $F_{1/2}(\eta)$  used to describe electron density in a semiconductor. *Solid-St. Electron.*, 25(11):1067–1076, Nov. 1982.
- [26] I-H. Tan, G. L. Snider, L. D. Chang, and E. L. Hu. A self-consistent solution of Schrödinger-Poisson equations using a nonuniform mesh. *J. Appl. Phys.*, 68(8):4071–4076, Oct. 1990.
- [27] X. H. Wang, B. Y. Gu, and G. Z. Yang. Coupling between normal and lateral degrees of freedom of an electron in quantum wells and superlattices at zero and finite magnetic fields. *Phys. Rev. B*, 56(15):9224–9227, Oct. 1997.
- [28] S. Khan-ngern and I. A. Larkin. Nonequilibrium electrons in double quantum well structures: a boltzmann equation approach. *Phys. Rev. B*, 64(11):115313, Aug 2001.